

Results of a search for the two neutrino double β decay of ^{136}Xe with proportional counters

Ju. M. Gavriljuk, V. V. Kuzminov,* and N. Ya. Osetrova
Institute for Nuclear Research, Moscow 117312, Russia

S. S. Ratkevich[†]
Kharkov State University, Kharkov 310077, Ukraine
 (Received 11 August 1999; published 14 February 2000)

Results of a search for ^{136}Xe double β decay with high-pressure multiwire wall-less proportional counters at the Baksan Neutrino Observatory are presented. The experimental method and the characteristics of the detectors are described. The detector background in the energy range 0.5–3.5 MeV has been reduced due to event position discrimination and pulse shape discrimination. Results of the analysis of background components for different event types and source positions are described. A new lower limit of $T_{1/2} \geq 0.81 \times 10^{21}$ yr (90% C.L.) is found for the ^{136}Xe $2\nu\beta\beta$ decay mode.

PACS number(s): 23.40.Bw, 27.60.+j, 29.40.Cs

I. INTRODUCTION

A search for the different modes of ^{136}Xe ($Q = 2.48$ MeV) double β decay is presented in Refs. [1–4]. Xenon was used as a working gas and double β decay source simultaneously in the different gas and liquid detectors. The types of detectors, working media, and results are summarized in Table I. A comparison of the results shows that the setup sensitivity to neutrinoless double β decay has been increased more than 200 times. This progress was achieved by lowering the background in the energy range 1.6–3.0 MeV by separating the two electron events [5]. The setup sensitivity to ^{136}Xe in the two neutrino double β decay mode has not changed substantially. Limits on the half-life of the ^{136}Xe $2\nu\beta\beta$ decay mode listed in Table I were established mainly by the analysis of spectra obtained after subtraction of the natural Xe spectrum from the spectrum of xenon enriched with ^{136}Xe in the energy range of 0.8–2.0 MeV in Refs. [2,3]. In Ref. [5] the limit was obtained by the analysis of the background spectrum only in the energy range of 1.67–2.0 MeV.

Theoretical predictions for the half-life of the ^{136}Xe $2\nu\beta\beta$ decay mode are $T_{1/2} = 0.82 \times 10^{21}$ yr [7], $T_{1/2} = 1.0 \times 10^{21}$ yr [8], $T_{1/2} = 4.64 \times 10^{21}$ yr [9]. To reach the level of the theoretical half life, it is necessary to increase the experimental sensitivity by 2–10 times.

II. EXPERIMENTAL SETUP

The main features of the new experimental setup that enables one to obtain a sensitivity to ^{136}Xe $2\nu\beta\beta$ decay of better than 8×10^{20} yr are described in [10]. This increase in sensitivity is achieved by using a multidetector measurement scheme which allows testing samples of natural xenon and xenon enriched in ^{136}Xe simultaneously. This scheme makes it possible to reduce the systematic errors related to variations of experimental external conditions. The detector is a

high-pressure multiwire wall-less proportional counter (MWPC) which consists of a central main counter (MC) and a surrounding protection ring counter (RC) in the same body. Detectors of similar construction are widely used for low background measurements with gaseous radioactive sources (see, for example, Refs. [11] and [12]). The diameters of the inner detector, RC anode grid, common MC and RC cathode grid are 122, 110, and 98 mm, respectively. The volumes of MC and RC are 4.44 and 2.57 l, respectively. The working pressure of xenon is 16.8 atm.

An increase of pulse amplitude due to gas amplification allows signals to be read from both ends of the MC anode (PC1 and PC2 signals). A parameter $\beta \equiv \text{PC1} \times 100 / (\text{PC1} + \text{PC2})$ determines the event coordinate along the detector. The selection of events inside the working anode length enables one to eliminate the background spectrum components related to microdischarges in the high voltage circuits and the insulator surfaces. The MC background component, related to the charged particles (electrons from radioactive impurities and external γ rays), is eliminated by an anticoincidence operation of the MC and RC (PAC signal). The MC event amplitude is formed as a sum of signals (PC1+PC2). A shaping amplifier with 26 μs integration and differentiation shaping times was used to obtain adequate energy resolution. The signals from the outputs of a nonshaping amplifier are joined together. The resulting signal, P12, is amplified in another shaping amplifier with $\tau_{\text{int}} \approx 0$ and $\tau_{\text{dif}} = 0.75 \mu\text{s}$.

The parameter $f \equiv \text{P12} \times 100 / (\text{PC1} + \text{PC2})$, depending on pulse rise time, is used to obtain its relative value. These data help to reduce the α -particle background.

Measurements were done in the underground laboratory of the Baksan Neutrino Observatory at 4900 m.w.e. depth. The experimental setup consists of three MWPC's installed in the low background shield (15 cm of lead, 8 cm of borated polyethylene and 11 cm of copper). The MWPC No. 1 was filled with a natural xenon without radioactive ^{85}Kr ; MWPC Nos. 2 and 3 were filled with xenon isotopically enriched in ^{136}Xe to 93%. The gases in the counters No. 1 and No. 2 were periodically purified and replaced. MWPC No. 3 was used as a control detector to expose the possible sources of

*Electronic address: kuzminov@neutr.novoch.ru

[†]Electronic address: ratkevich@univer.kharkov.ua

TABLE I. The detector characteristics and experimental results of the search for the zero- and two-neutrino modes of the ^{136}Xe double β decay.

Detector, volume (l) pressure (atm)	Sample enriched ^{136}Xe	Number of atoms ^{136}Xe	$T_{1/2}$ yr (C.L.) $2\nu\beta\beta$	$T_{1/2}$ yr (C.L.) $0\nu\beta\beta$
Ionization chamber 3.66 l 20–30 atm	^{136}Xe , 93%	2.14×10^{24}	$\geq 2.7 \times 10^{20}$, 68% [2]	$\geq 3.3 \times 10^{21}$, 68% [1]
	$^{\text{nat}}\text{Xe}$, 9.2%	2.12×10^{23}		
	^{136}Xe , 64%	1.24×10^{25}	$\geq 2.9 \times 10^{20}$, 84% [3]	
Multisection proportional counter 79.4 l 9.7 atm			$\geq 1.6 \times 10^{20}$, 95% [3]	$\geq 1.2 \times 10^{22}$, 95% [3]
	^{136}Xe , 93%	3.6×10^{24}		$\geq 2.4 \times 10^{21}$, 68% [4]
	^{136}Xe , 62%	1.46×10^{25}	$\geq 2.1 \times 10^{20}$, 90% [5] $\geq 3.6 \times 10^{20}$, 90% [6]	$\geq 6.9 \times 10^{23}$, 68% [5] $\geq 4.4 \times 10^{23}$, 90% [6]
Liquid scintill. counter 0.313 l TPC 180 l 5.0 atm MWPC 4.44 l 17.8 atm	^{136}Xe , 93%	2.14×10^{24}	$\geq 1.33 \times 10^{21}$, 68%	
			this paper	
	$^{\text{nat}}\text{Xe}$, 9.2%	1.96×10^{23}	$\geq 0.81 \times 10^{21}$, 90%	

systematic errors related to a gas exchange in the MWPC Nos. 1 and 2. Energy calibration was done with ^{137}Cs (662 keV), ^{54}Mn (835 keV) and ^{22}Na (1275 keV) γ -ray sources. The energy resolutions of these γ lines were 10%, 8.8% and 6.3%, respectively, for the spectra of signals (PC1+PC2) without the signal PAC (type-I events). The ^{40}K and ^{232}Th γ -ray sources, uniformly distributed along the detector length, were used for the complex calibration. Type-I amplitude spectra of these sources for MWPC No. 3 are presented in Fig. 1. For convenience of the data presentation in the logarithmic scale we added 1 to the number of counts in each

spectrum channel. The ^{40}K and ^{232}Th spectra were obtained with 35 and 226 h of measurement time, respectively. Similar spectra of MWPC Nos. 1 and 2 have different shapes because of the pulses related to the microdischarges of the high voltage circuits. Type-I event distributions for MWPC Nos. 1, 2, 3, along the β axis, for ^{40}K γ -ray calibration in the energy range of $E \geq 600$ keV, are shown in Fig. 2. One observes peaks in the β distributions MWPC Nos. 1 and 2 which are not related to the γ -ray sources. Intensities of the peaks change in time and correlate with the humidity in the laboratory. In the range $f \leq 150$ the f -distribution shapes are

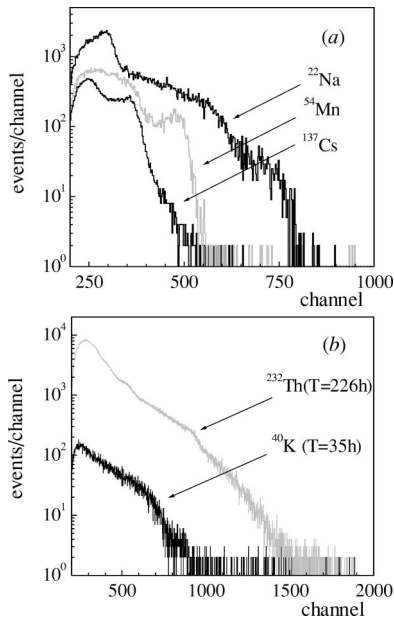


FIG. 1. The spectra of the PC1+PC2 signals in the type-I events for MWPC No. 3 calibrated with ^{137}Cs , ^{54}Mn , ^{22}Na , ^{40}K , ^{232}Th sources.

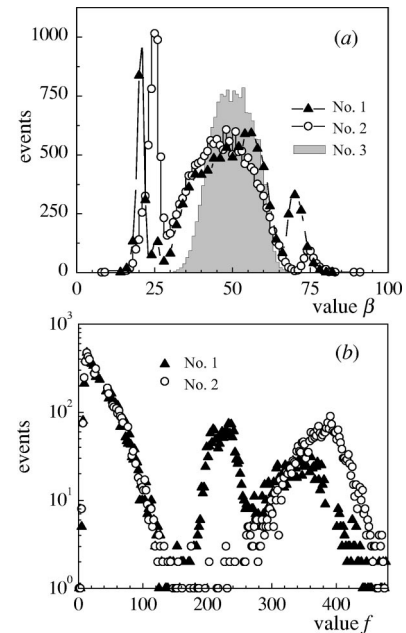


FIG. 2. The distributions of the type-I events with energies above 600 keV (^{40}K) in MWPC Nos. 1, 2, and 3, in value of the parameters β (a) and f (b).

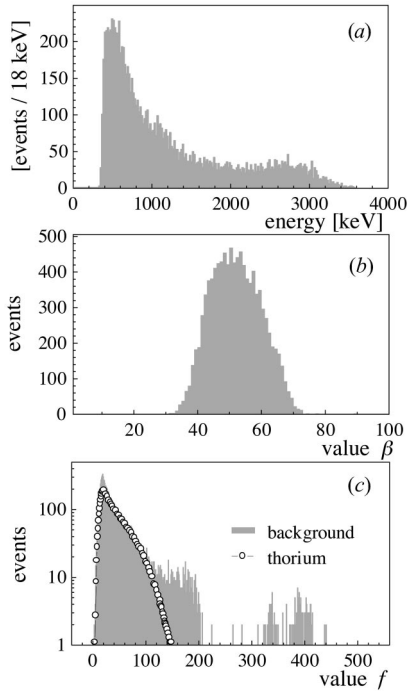


FIG. 3. The distributions of the background type-I events in MWPC No. 3 (a) in the energy value and values of parameters β (b) and f (c). The f distributions for the ^{232}Th spectrum from Fig. 1 for MWPC No. 3 (normalized to the exposure time) present in (c). The exposure time was 730.5 h.

the same. In the distributions for MWPC Nos. 1 and 2 there are peaks at high f which are not related to the γ -ray source. The cut $1 \leq f \leq 150$ enables one to eliminate the peaks in the β distributions which are outside of the working region of the detector and to obtain the coincidence of the ^{40}K spectra for the three counters.

III. RESULTS

Experimental data of the search for the $^{136}\text{Xe } 2\nu\beta\beta$ decay mode have been obtained during four runs of 1358.8, 1085.4, 730.5, and 1106.0 h using MWPC Nos. 1 and 2. The MWPC No. 1 was filled with ^{136}Xe during the first and third runs (the total data-acquisition time was 2089.3 h) and with $^{\text{nat}}\text{Xe}$ during the second and fourth runs (total data-acquisition time was 2191.4 h). The gas-filling sequence for the MWPC No. 2 was opposite. As was noted above, MWPC No. 3 was used as a control detector. Accidentally, it had no pulses related to the microdischarges at high voltage circuits. The experimental spectrum, β , and f distributions for this detector allowed a correct interpretation of the data from MWPC Nos. 1 and 2.

A MWPC No. 3 background spectrum of type-I events, collected for 730.5 h and corresponding β (b) and f distributions (c), are shown in Fig. 3. The normalized f distribution of ^{232}Th spectrum (Fig. 1) at energies above 600 keV is shown in Fig. 3(c). By comparing the f distributions for background events with that of the ^{232}Th source, one can see that events with leading edges larger than those for electrons (larger values of f) are present in the background spectrum. These events may be caused by α particles from decay of

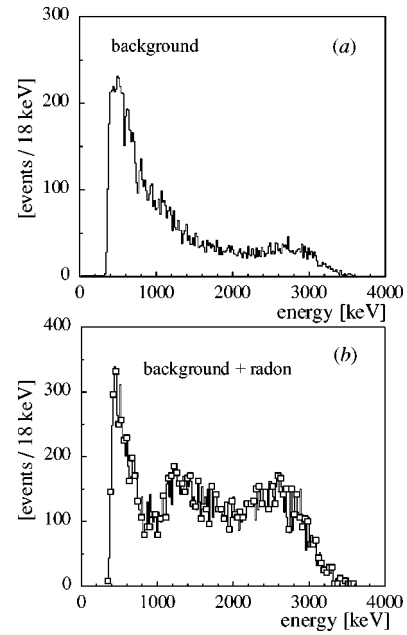


FIG. 4. The background spectrum in MWPC No. 3 over 140 h before (a) and after (b) radon addition.

^{222}Rn in the gas ($T_{1/2}=3.82$ day, $E_{\alpha}=5.49$ MeV) and its daughter nuclei— ^{218}Po ($T_{1/2}=3.05$ min, $E_{\alpha}=6.0$ MeV) and ^{214}Po ($T_{1/2}=1.64 \times 10^{-4}$ s, $E_{\alpha}=7.69$ MeV)—at the electrode surfaces where they are deposited, having been produced as charged ions. Moreover, α particles can be emitted in the decays of the isotopes from the uranium and thorium series, which are included as impurities in materials of the cathode and anode wires. A sample of ^{222}Rn was introduced in MWPC No. 3 to define the α -particle background spectrum of ^{222}Rn and its daughter isotopes.

The MWPC No. 3 background spectra before (a) and after (b) the input of the radon are shown in Fig. 4. Counting periods were 140 h in both cases. Spectrum (a) has a uniform event distribution in time, spectrum (b) is an exponential with $T_{1/2} \approx 4$ days superimposed on a constant base. By comparing the background (a) and radon (b) spectra, one observes that the MWPC background at $E \geq 1300$ keV is caused by equilibrium ^{222}Rn decays which are constantly present in the working gas. Radon can be generated in the structural materials inside the counter. An energy-scale discrepancy for electrons and α particles is caused by an incomplete ionization collection from the α -particle tracks at the gas pressure and electric-field strengths used.

The f distributions in the energy ranges of 1240–1640 keV (curve 1) and 2740–3120 keV (curve 2) for radon decays are shown in Fig. 5. From the distribution of the spectrum in the second energy range, one observes that the pulses have a wide spread in rise time with a weak maximum at $f \approx 140$. There are several causes to explain this distribution. First, the ionization collection time for a track with the same length of its projection onto the radius in the inhomogeneous counter field depends on the distance to the anode. The estimate made with the data [13] shows that, under given conditions, for a track with 5 mm projection length, the time of electron deposition on the anode is 18.7 and 5 μs at a mini-

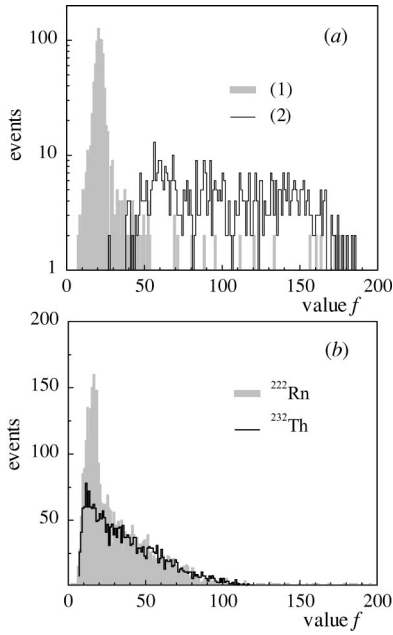


FIG. 5. The event distribution in the value of f : (a) for events from radon decay in energy ranges of (1) 1240–1640 keV and (2) 2740–3120 keV; (b) for events with 600–1160 keV energies from the background spectra of Fig. 4(a) and of the ^{232}Th source.

mal track-to-anode distance of 25 and 10 mm, respectively (ignoring the track spreading through electron diffusion during the drift). Therefore, the larger the distance from the radon decays to the anode, the longer the leading-edge time for the α particle. In addition, this time depends on track orientation. Second, since daughter ^{218}Po is produced as a positive ion, it is deposited in the electric field on the cathode grid or anode, respectively. Pulses from α particles emitted in the ^{218}Po and ^{214}Po decays on the anode have minimal values of rise time and maximal values of parameter f . The peak at $f \approx 140$ in the f distribution [Fig. 5(a), curve 2] probably correspond to these decays. The α -particle pulses from the ^{218}Po and ^{214}Po decays on the cathode have the longest rise time and the smallest height, because, at low electric intensity near the cathode grid, the conditions of the ionization collection from a dense track deteriorate and the probability of the charge recombination increases. Since the distance from the anode to such decays is fixed, the leading edges have a relatively small spread. For this reason there is a pronounced peak in the f distribution at $f=20$. There are f distributions shown in Fig. 5 for events corresponding to the energy range 600–1160 keV for background spectrum and of the ^{232}Th spectrum. By comparing these distributions one observes the excess events with a long rise time. Possibly this excess is caused by the α decays of uranium and thorium isotopes in the cathode grid wires, and by radon decay in the border region between MC and RC.

The β and f distributions of the events in the MWPC Nos. 1 and 2 obtained during the third counting period of the background measurement are shown in Fig. 6. Comparing these distributions with the corresponding distributions of events for MWPC No. 3, one observes components of a background spectrum related to microdischarges in the high-

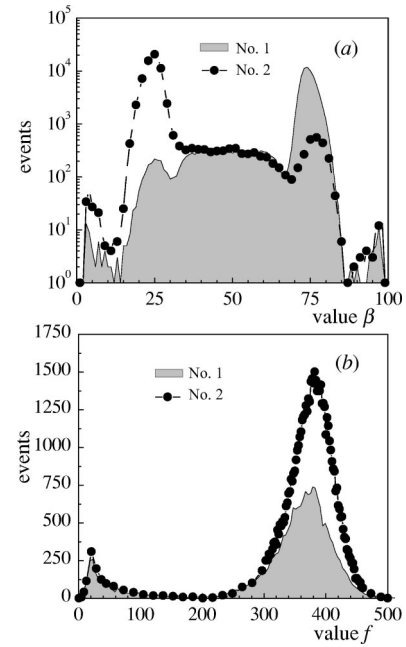


FIG. 6. The β and f distributions of the events in MWPC Nos. 1 and 2, stored up in the background measurements in the third counting period (730.5 h).

voltage output circuits. These events are concentrated in the side peaks in the range $f \geq 200$. Selection of events with the parameter f ranging from 1 to 200 out of the total spectrum results in the disappearance of the side peaks in the β distributions (see Fig. 7).

The counting rates are 2.08 and 2.47 h^{-1} for the energy ranges of 700–1000 keV and 1000–2000 keV, respectively. Type-II event counting rates (MC pulses in coincidence with

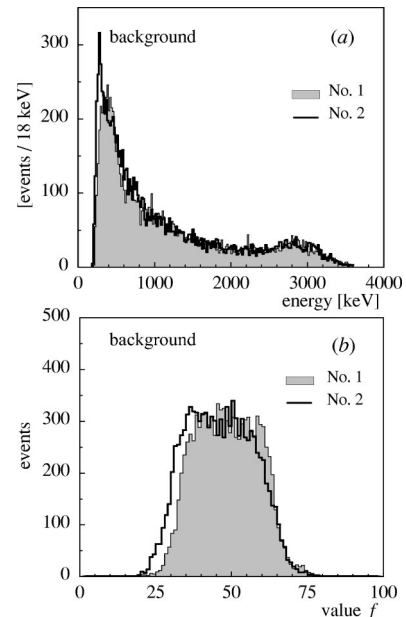


FIG. 7. The distributions of events with f -parameter values $1 \leq f \leq 200$ in (a) energy and (b) β parameter for MWPC Nos. 1 and 2.

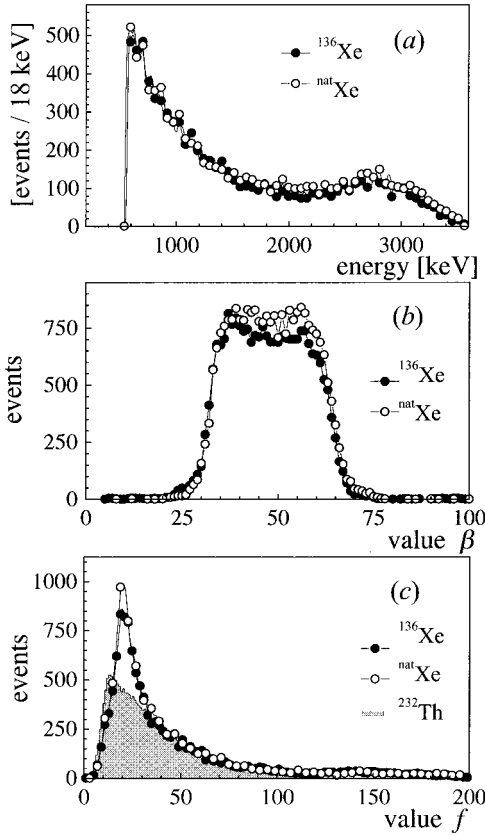


FIG. 8. The final total distributions of events with f in range from 1 to 200: (a) total background spectrum of MWPC Nos. 1 and 2 when filled with ^{136}Xe and $^{\text{nat}}\text{Xe}$; (b,c) β and f distributions of the events with energies above 700 keV for ^{136}Xe and $^{\text{nat}}\text{Xe}$, normalized f distribution of thorium events with 700–1800 keV energies in the MWPC No. 2.

RC pulses) are 1.34 and 0.39 h^{-1} , respectively, for the ranges mentioned above. For MWPC placed in the surface laboratory (i.e., without low underground shield) the background counting rates are 6557 and 3212 h^{-1} for type-I events and 2315 and 1250 h^{-1} for type-II events, respectively.

The experimental data in the energy range of 700–1800 keV were obtained during four counting periods (4280.7 h) and were summarized for each counter to compare their own background. The range of $30 \leq f \leq 130$ was used to exclude the microdischarges and α -particle events. The number of events 3829 and 3800 were obtained for MWPC Nos. 1 and 2, respectively. One observes that background spectra of counters are in agreement within one standard error (1σ). This result enables one to sum the spectra for each gas separately to reduce the systematic errors due to design features of the counters.

The total background spectra for counters filled with ^{136}Xe and $^{\text{nat}}\text{Xe}$ in the energy range of $E \geq 700 \text{ keV}$ and $1 \leq f \leq 200$ and the f and β distributions corresponding to these spectra are shown in Fig. 8. In Fig. 8(c) there is a normalized f distribution taken with a ^{232}Th source in the energy range of 700–1800 keV for the MWPC No. 2. One

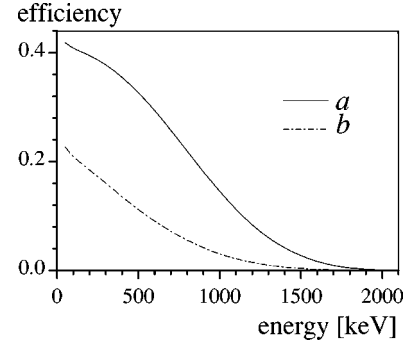


FIG. 9. The total detection efficiency in the central counter for the two-neutrino double β decay of ^{136}Xe as the type-I and type-II events.

observes that the working range for f does not exceed the value of 138. The α -particle events born near the cathode grid lie in the range of $1 \leq f \leq 21$. In this range, the f distribution of ^{136}Xe differs slightly from the f distribution of $^{\text{nat}}\text{Xe}$ and both of them differ essentially from the f distribution of ^{232}Th . A small excess of α particles in the spectrum of $^{\text{nat}}\text{Xe}$ presented in Fig. 8(b), in comparison with the spectrum of ^{136}Xe , can be explained by the fact that natural xenon was the first working gas in the procedure of collection and purification of gases. In the final data analysis, it was found that the level of the radon impurities from the Ti getter was higher for $^{\text{nat}}\text{Xe}$ than for ^{136}Xe which was the second gas to be purified and collected. The events from the region $21 \leq f \leq 138$, for the energy range of 700–1800 keV were included in the final analysis to eliminate the α -particle background. The fraction of electron events excluded with this cut was determined by using a ^{232}Th source f distribution as the efficiency ϵ_1 of a selection procedure. The number of events for the ^{136}Xe -filled detector was 10 428, while the number of events for the $^{\text{nat}}\text{Xe}$ -filled detector was 10 512. The counting rates are $n_1 = 2.436 \pm 0.024 \text{ h}^{-1}$ and $n_2 = 2.455 \pm 0.024 \text{ h}^{-1}$, respectively. The difference of the counting rate values is $\Delta n = n_1 - n_2 = -0.019 \pm 0.034 \text{ h}^{-1}$ or $\Delta n = -166 \pm 298 \text{ yr}^{-1}$. Since this value does not exceed 1σ , there is an expression for the limit on the half-life of the ^{136}Xe $2\nu\beta\beta$ decay mode:

$$T_{1/2}(2\nu, 0^+ - 0^+) \geq \ln 2 \times \epsilon_1 \times \epsilon_2 \times N_0 / \sigma, \quad (1)$$

where $\epsilon_1 = 0.754$ is the efficiency of selection; ϵ_2 is the efficiency for detection of $2\nu\beta\beta$ decay events; $\sigma = 298 \text{ yr}^{-1}$ is the experimental standard error; N_0 is the difference of the number of ^{136}Xe atoms in the counters with enriched and natural samples of xenon. $N_0 = (\eta_1 - \eta_2) \times (V/V_\mu) \times (P/\rho) \times N_a = 2.99 \times 10^{24}$; $\eta_1 = 0.93$ and $\eta_2 = 0.092$ are the contents of the ^{136}Xe atom in the enriched and natural samples of xenon, respectively; $V = 7.9121$ is the total volume of the counter where electrons reach the MC working region; $V_\mu = 22.41$ is a volume of one gas mole at NTP ; $P = 16.3 \text{ atm}$.

is the working gas pressure; $\rho=0.97$ is the compression coefficient for xenon at $P=16.3$ atm and $T=293$ K; $N_a=6.02\times 10^{23}$ is Avogadro's number.

The efficiency of the detection of $2\nu\beta\beta$ decay events was calculated by Monte Carlo simulation of the electron trajectories taking into account the counter end and wall effects. The dependences of the total efficiency (number of events of the given type with an amplitude higher than the specified one, referred to the total number of events of the double β decay) for events of the types I and II are presented in Fig. 9. The detection efficiency ϵ_2 for type-I events in the 700–1800 keV energy range is equal to 0.254. After the substitution of all values into expression (1) we have

$$T_{1/2}(2\nu,0^+-0^+)\geq 1.33\times 10^{21}\text{ yr (68\% C.L.) or,}$$

$$T_{1/2}(2\nu,0^+-0^+)\geq 0.81\times 10^{21}\text{ yr (90\% C.L.).}$$

ACKNOWLEDGMENTS

This work was supported by the Russian Fundamental for Basic Research (Grant No. 93-02-15499), and that part concerning the development of methods for active background suppression in large proportional counters by the International Science Foundation (Grant No. RNT000), and the RF Government (joint project with the International Science Foundation, No. RNT300).

-
- [1] A. S. Barabash *et al.*, *Sov. J. Nucl. Phys.* **51**, 1 (1990).
 [2] V. V. Kuzminov *et al.*, *Proceedings of the International Moriond Workshop, Massive Neutrinos, Test of Fundamental Symmetries* (Editions Frontieres, Paris, 1991), p. 105.
 [3] E. Bellotti *et al.*, *Phys. Lett. B* **266**, 193 (1991).
 [4] I. Barabanov *et al.*, *Pis'ma Zh. Eksp. Teor. Fiz.* **43**, 116 (1986).
 [5] V. Jorgens *et al.*, *Nucl. Phys. B (Proc. Suppl.)* **35**, 378 (1994).
 [6] R. Luescher *et al.*, *Phys. Lett. B* **434**, 407 (1998).
 [7] J. Engel, P. Vogel, and M. Zirubaner, *Phys. Rev. C* **37**, 731 (1988).
 [8] O. Rumjantsev and M. Urin, *Phys. Lett. B* **443**, 51 (1998).
 [9] A. Staudt, K. Muto, and H. V. Klapdor-Kleingrothaus, *Europhys. Lett.* **13**, 31 (1990).
 [10] G. Volchenko *et al.*, *Instrum. Exp. Tech.* **42**, 1, 34 (1999).
 [11] V. V. Kuzminov, A. A. Pomansky, and P. S. Striganov, *Nucl. Instrum. Methods Phys. Res.* **203**, 477 (1982).
 [12] V. V. Kuzminov, N. Ya. Osetrova, and A. M. Shalagin, *Instrum. Exp. Tech.* **39**, 5, 654 (1996).
 [13] A. Peisert and F. Sauli, Drift and diffusion of electrons in gases a compilation, Internal Report CERN-EP/84-08, 1984.